



Research on underwater imaging technology based on polarization difference

Li Xu¹ · Yuhang Li¹

Received: 23 July 2023 / Accepted: 21 October 2023
© The Author(s), under exclusive licence to The Optical Society of India 2023

Abstract Traditional underwater polarization differential imaging methods use a fixed polarization direction to suppress the background scattered light; however, the polarization angle of the background scattered light may change in different underwater environments, limiting their effectiveness and real-time performance. In this paper, an improved underwater polarization differential imaging method is proposed, in which the polarization angle with the highest frequency of occurrence is selected as the polarization angle of the backscattered light by Stokes vector analysis. Then, the polarization images of the two best orthogonal polarization directions are obtained by combining the polarizer Mueller matrix and processed differentially. Compared with the traditional method, this method can suppress the backscattered light more accurately and effectively and improve the quality and real-time performance of underwater imaging. This method will have an important impact on imaging applications in complex underwater scenes.

Keywords Scattering · Polarization · Stokes vector · Polarization difference · Polarization angle

Introduction

In recent years, underwater optical imaging technology has been widely used in the fields of underwater target detection, environmental monitoring, and ocean exploration. However,

due to the influence of the underwater turbid medium, the underwater target signal light will be obscured by the background scattered light, resulting in a degradation of imaging quality. This problem seriously affects the accuracy and reliability of underwater detection and monitoring, and also negatively affects the real-time and imaging effects of underwater imaging systems. Therefore, the main difficulties that need to be solved in underwater imaging are to remove the background scattered light, restore a clear underwater scene, and enhance the imaging contrast and clarity [1].

In the process of underwater imaging, backscattered light is the main cause of poor imaging quality. For a long time, researchers at home and abroad have proposed various methods and techniques to minimize the effect of this scattering. For example, time gating [2, 3], acoustic imaging [4], super-resolution fusion [5], and ghost imaging [6]. However, all of these techniques suffer from the disadvantages of large mass, complex and cumbersome systems, and high costs, making it difficult to apply them to complex underwater environments. In contrast, polarization imaging techniques have attracted much attention due to their simple hardware, practical operation, and low price [1]. The polarization imaging technique realizes clear underwater imaging by analyzing the polarization state of the target and the background to reflect the light intensity changes of the target signal light and the background scattered light and suppressing the influence of the background scattered light. The polarization imaging method can provide richer target information, which is a popular research direction in underwater imaging.

Common polarization imaging methods include polarization filters, polarization rotators, and polarization differential imaging, among which polarization differential imaging techniques are widely used in the field of optical imaging. The traditional polarization imaging method is to acquire two mutually orthogonal polarization images by

✉ Li Xu
xuli@ncwu.edu.cn

¹ School of Electronic Engineering, North China University of Water Resources and Electric Power, Zhengzhou 450000, Henan, China

changing the polarization angle of the polarization detector in an unordered manner [7], and these images are processed differentially to improve the contrast of the target signal. However, this method has some limitations, such as taking a lot of time to acquire multiple polarization images, which reduces the real-time performance of imaging [8]; moreover, in an underwater environment with strong scattering, the traditional polarization differential imaging method is still unable to effectively enhance the contrast and details of the images. To address the above problems, this paper proposes an improved underwater polarization differential imaging method, which uses the Stokes vector to calculate the polarization angle of the background scattered light, and then selects the best two mutually orthogonal polarization directions to differentiate the image. Compared with the conventional method, this method does not require a rotating detector, which improves the real time and efficiency of imaging. In addition, the method utilizes the polarization information of the background scattered light to determine the optimal combination of the polarization directions, which can effectively reduce the influence of the background scattered light on the imaging results and thus enhance the contrast and details of the image.

To verify the effectiveness of the method in this paper, a series of experiments were conducted and compared with the traditional polarization differential imaging method. The experimental results show that the improved underwater polarization differential imaging method proposed in this paper can significantly improve the clarity and contrast of images in a strong scattering underwater environment, effectively reduce the interference of the background scattered light, and at the same time have high real-time performance and imaging effect.

Theory

Principle of polarization difference imaging

In the process of underwater detection, the detector receives light partly from the backscattered light reflected by the scattering medium and partly from the target signal light reflected from the object. Polarization differential imaging uses two mutually orthogonal polarized images for the difference to obtain the image. It utilizes the difference in vibration direction between the two light vectors to eliminate the background scattered light [9]. Figure 1 shows the physical model of the polarization difference method [10],

where T is the target signal light, B is the background scattered light, and $P1$ and $P2$ are the transmittance axes in both directions.

As shown in Fig. 1, assuming that the background scattered light and the target signal light are perfectly linearly

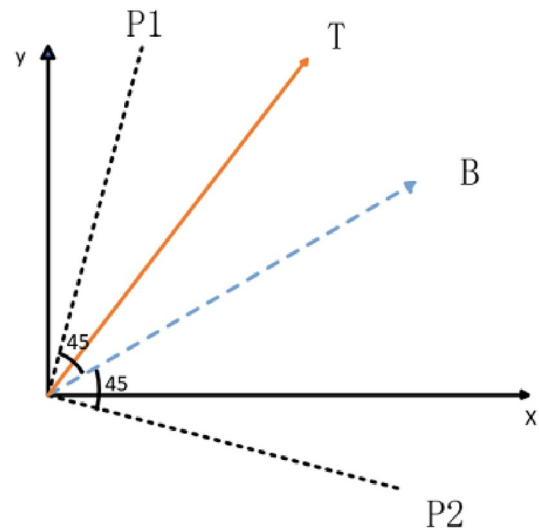


Fig. 1 Polarization differential imaging schematic

polarized, the direction of the transmission axis is set at $\pi/4$ to the direction of the background scattered light, and two polarization images with orthogonal polarization directions are acquired and differenced to obtain Eq. (1).

$$I_{pd} = I(0) - I(90) = [T(0) + B(0)] - [T(90) + B(90)] \quad (1)$$

Here, 0 and 90 represent the two directions of the transmission axis $P1$ and $P2$, respectively. Since the angle between the transmission axis and the background scattered light is $\pi/4$, the intensity of the background scattered light in both directions can be determined according to Marius' law [11]

$$B(0) = B(90) = \frac{B}{2} \quad (2)$$

Substituting Eq. (2) into Eq. (1),

$$I_{pd} = T(0) - T(90) \quad (3)$$

A comparison of Eqs. (1) and (3) shows that the background scattered light is removed, while the target signal light is retained.

Principle of underwater imaging based on polarization difference.

Stokes vector is the mainstream method to characterize the polarized light, the Stokes vector of the beam can be calculated from the polarization images of the four polarization directions of 0° , 45° , 90° , and 135° , and the intensities of these four images can be expressed as $I(0)$, $I(45)$, $I(90)$, and $I(135)$, respectively, and then the stokes vector can be expressed as Eq. (4) [12, 13]

$$S = \begin{bmatrix} S_0 \\ S_1 \\ S_2 \end{bmatrix} = \begin{bmatrix} I(0) + I(90) \\ I(0) - I(90) \\ I(45) - I(135) \end{bmatrix} \quad (4)$$

Here, S_0 denotes the total light intensity, S_1 denotes the difference in light intensity between the horizontal and vertical line polarization components, and S_2 denotes the difference in light intensity between the 45° and 135° line polarization components [14]. Then, the angle of polarization (AOP is denoted by θ) can be expressed as Eq. (5) [15, 16].

$$\theta = \frac{1}{2} \arctan \frac{S_2}{S_1} \quad (5)$$

The Mueller matrix is usually used to describe the polarization information of an object, and when the angle between the transmission axis of the polarizer and the horizontal direction is α , the corresponding Mueller matrix of the polarizer is Eq. (6). [17, 18]

$$M = \frac{1}{2} \begin{bmatrix} 1 & \cos 2\alpha & \sin 2\alpha \\ \cos 2\alpha & \cos^2 2\alpha & \sin 2\alpha \cos 2\alpha \\ \sin 2\alpha & \sin 2\alpha \cos 2\alpha & \sin^2 2\alpha \end{bmatrix} \quad (6)$$

Knowing the Stokes vector of a beam of light and the Mueller matrix of the polarizer, the Stokes vector of this beam of light when it passes through the polarizer is Eq. (7)

$$S_{\text{out}} = M \cdot S_{\text{in}} \quad (7)$$

From Eq. (7), when the Stokes vector of light and the Mueller matrix of the polarizer are known, the Stokes vector of light passing through any angle of the transmissive axis can be found, and according to the physical meaning of the Stokes vector, combined with the Eq. (7), it can be obtained that the light intensity of light passing through the polarizer is

$$I_\alpha = \frac{1}{2} (S_0 + S_1 \cos 2\alpha + S_2 \sin 2\alpha) \quad (8)$$

Through Equation $S_0 = I(0) + I(90)$, it is known that S_0 contains both target signal light and scattered light, while S_1 and S_2 are almost unaffected by the target signal light, so according to Eq. (5), it is known that the polarization angle AOP can provide more accurate information about the scattered light [19].

Different from the traditional polarization difference method, the method proposed in this paper does not need to rotate the angle of the polarizer but to find out the polarization angle image through formula (5), based on which the polarization angle with the highest frequency of occurrence is selected as the polarization angle of the scattered light and denoted by θ_A , and the polarization angle in the optimal mutually orthogonal direction is obtained through the

polarization angle of the scattered light. To eliminate the scattered light in the θ_A polarization direction, the polarization angle in the parallel direction is obtained according to the principle of polarization difference as

$$\theta_{\parallel} = \theta_A - \frac{\pi}{4} \quad (9)$$

The angle of polarization in the vertical direction is

$$\theta_{\perp} = \theta_A + \frac{\pi}{4} \quad (10)$$

Substituting Eqs. (9) and (10) into Eq. (8) yields two mutually orthogonal images I_{\parallel} and I_{\perp} of the optimal polarization direction, denoted respectively as

$$I_{\parallel} = \frac{1}{2} [S_0 + S_1 \cos 2\theta_{\parallel} + S_2 \sin 2\theta_{\parallel}] \quad (11)$$

$$I_{\perp} = \frac{1}{2} [S_0 + S_1 \cos 2\theta_{\perp} + S_2 \sin 2\theta_{\perp}] \quad (12)$$

According to the conventional polarization difference principle, we have

$$I_{\text{pd}} = I_{\parallel} - I_{\perp} \quad (13)$$

Substituting Eqs. (11) and (12) into Eq. (13) yields

$$I_{\text{pd}} = S_1 \sin 2\theta_A - S_2 \cos 2\theta_A \quad (14)$$

Equation (14) is the result obtained by our method. This method utilizes Stokes vectors to calculate the polarization angle, which increases the real-time performance of underwater imaging. And the polarization angle with the highest frequency of occurrence in the AOP image is used as the estimation of the backscattered light, which can be filtered out most of the backscattered light by the difference, increasing the effectiveness of underwater imaging.

Experimental results and discussions

The experimental setup of polarization-based differential underwater imaging is shown in Fig. 2. The illumination source is the CEL-LED100HA high-power LED light source system. The LED lamp has a light output of 20W, a 55-mm-diameter light outlet, and a spot diameter adjustment of 30 mm using a condensing lens, which allows the light to pass through the polarizer. The light system also allows for fast and stable adjustment of the light output intensity, which can be used in underwater environments with varying levels of light and darkness. The LED lamp was chosen because of its ability to achieve high power output in a relatively small device, which makes it possible to transplant the polarization imaging system into the current underwater imaging

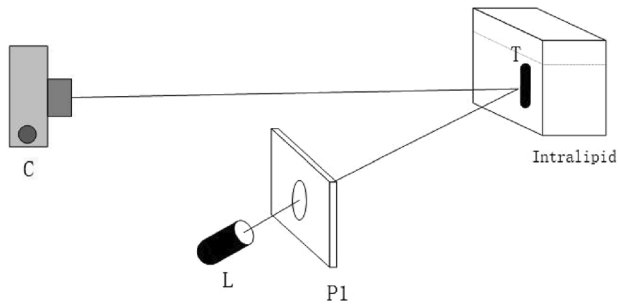


Fig. 2 Diagram of the experimental setup for underwater polarization imaging. P1 polarizer. C polarization camera. L light source. T target

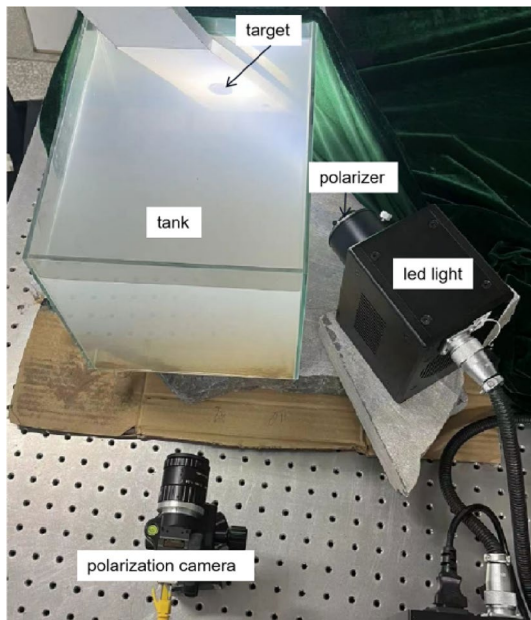
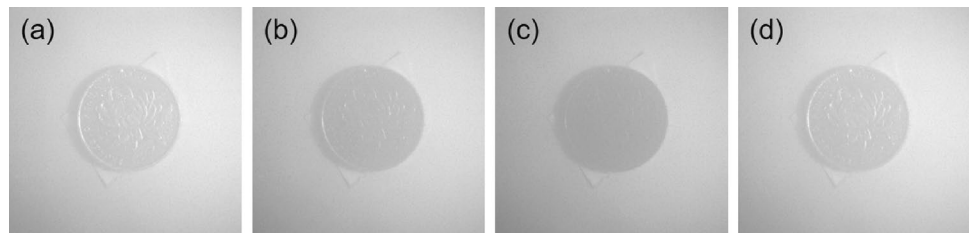


Fig. 3 Physical diagram of underwater polarization imaging experimental equipment

system. The camera model used in this experiment is the phx050s-pc polarization camera, which has four different angles of polarizers on the sensor placed on a single image element, allowing for the simultaneous acquisition of polarized images from four angles, which allows the system to be applied in dynamic environmental environments. Water is

Fig. 4 a, b, c, d Polarization images in 0° , 45° , 90° , and 135° directions, respectively



mixed with other scattering media in a glass tank to simulate an underwater scattering environment. The light output from the LEDs is transformed into fully linearly polarized light through a polarizer, which is then reflected by the target object and finally received by the detector. A diagram of our experimental equipment for underwater polarization imaging is shown in Fig. 3.

The algorithms in this paper are validated in the MATLAB 2022 software environment for underwater imaging.

According to the experimental setup in Fig. 2, firstly, to verify the effect of directly transmitted light and scattered light on the polarization angle AOP, a metal coin was chosen as the experimental object, which was glued to a plastic plate and immersed in water. Then, add milk to the water to make it turbid, and use the polarization camera to obtain the polarization images of the 0° , 45° , 90° , and 135° directions, respectively. As shown in Fig. 4(a–d), it can be seen that the visibility of the target is very low, and the detailed information of the object can hardly be seen under the turbid water.

The AOP image can be obtained through Eq. (5), as shown in Fig. 5a. It can be seen through the AOP image that there is a slight difference between the target and the surroundings, which means that the polarization direction of the target signal light is different from that of the scattered light. To be able to obtain the polarization direction of the scattered light more accurately, the polarization angle with the highest frequency of occurrence in the non-target region is selected as the estimated value of the polarization angle of the scattered light, as shown in the histogram of the polarization angle distribution in Fig. 5b.

These polarized images are then processed to verify the effectiveness of our method. The images recovered using our method are shown in Fig. 6c. Comparing Fig. 6c with Fig. 6a, it can be seen that the visibility of Fig. 6a is very low and the details of the object are hardly visible, while the visibility of the image in Fig. 6c is improved and the image quality is much better. The detailed information about the object is easier to distinguish, especially the flower pattern on the coin, which becomes clearer. This indicates that this method can effectively remove scattered light. In addition, we also compared the method in this paper with the difference method and light intensity difference method of Jinping Zhu's group [20], and the results of the two difference methods are shown in Fig. 6b and d. The comparison shows

that the method proposed in this paper has clearer images, more obvious details, and is superior in suppressing backward scattered light.

The change in image contrast can be visualized by a histogram. Figure 7(a–d) shows the histograms of Fig. 6(a–d), respectively. The gray-scale distribution of Fig. 7a is mainly concentrated in a narrow range, which means that the detailed information of the image is submerged, and the gray-scale distributions of Fig. 7b and d are widened compared with Fig. 7a, while the gray-scale distribution of Fig. 7c is much wider than that of Fig. 7(a, b and d). Therefore, Fig. 7c can be easily recognized with more details.

In this paper, three metrics, namely information entropy, standard deviation [21], and contrast, are used to quantitatively evaluate the image quality. The information entropy, standard deviation, and contrast corresponding to each image in Fig. 6 are given as shown in Table 1. As shown in Table 1, the information entropy, standard deviation, and contrast of the method proposed in this paper are significantly higher than those of other methods, which indicates that the image quality obtained by this paper’s method is higher, which coincides with the intuitive judgment of the recovery results of this paper’s method in Fig. 6.

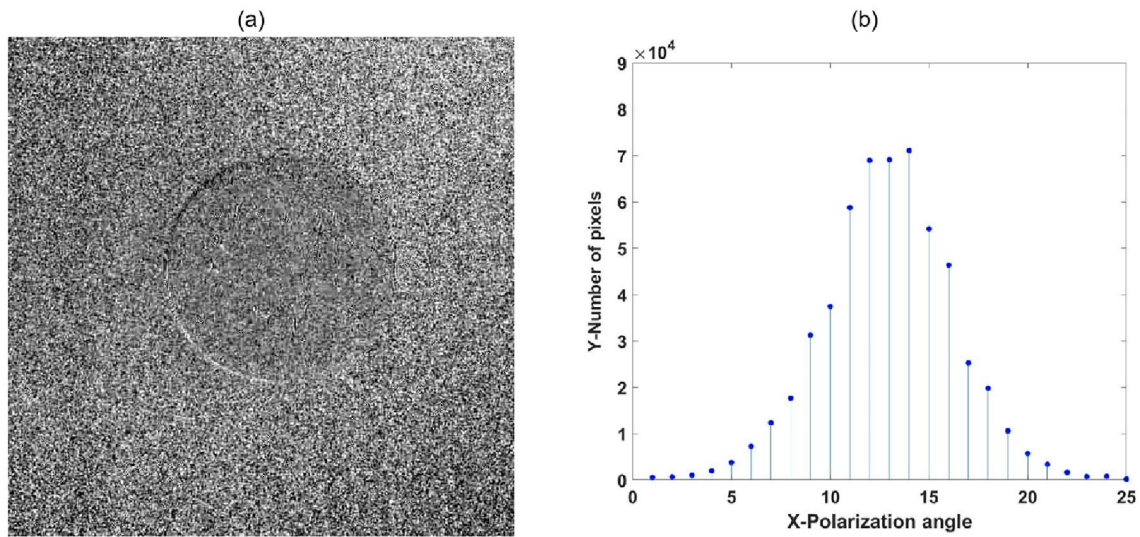


Fig. 5 **a** Polarization angle (AOP) image; **b** Histogram of polarization angle distribution

Fig. 6 Plot of the processing effect of different methods. **a** Raw image. **b** Image processed by intensity difference method. **c** Image processed by our method. **d** Image processed by Zhu’s method [20]

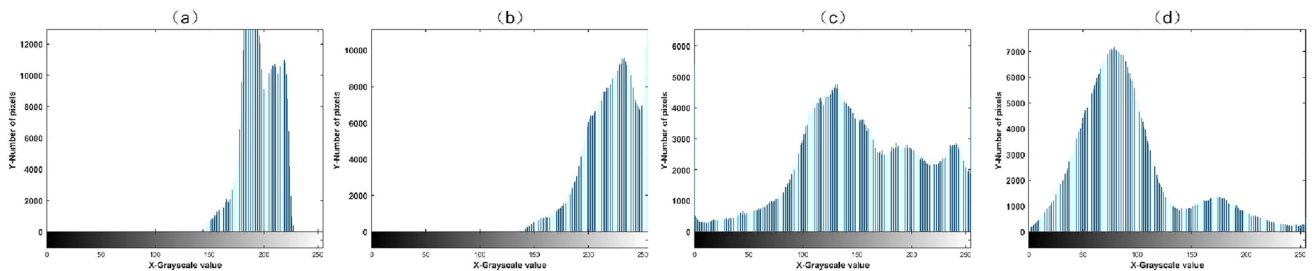
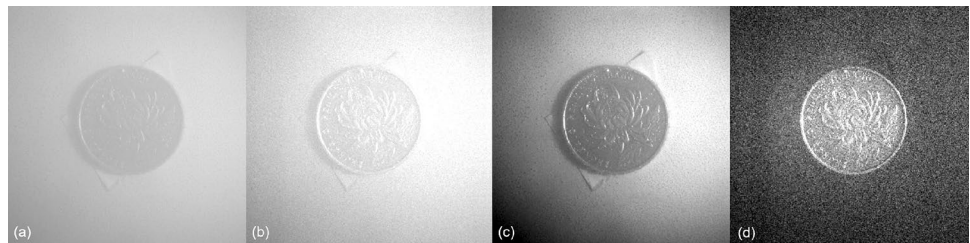


Fig. 7 **a–d** Histograms of Fig. 5 **a–d**, respectively

Table 1 Evaluation of image quality by different indicators

	Information entropy	Standard deviation	Contrast
Raw image	5.9239	15.9883	0.1514
Polarization difference	6.2702	24.0313	0.3043
Our method	7.6992	57.1964	0.7230
Zhu's method	6.4624	30.5063	0.6403

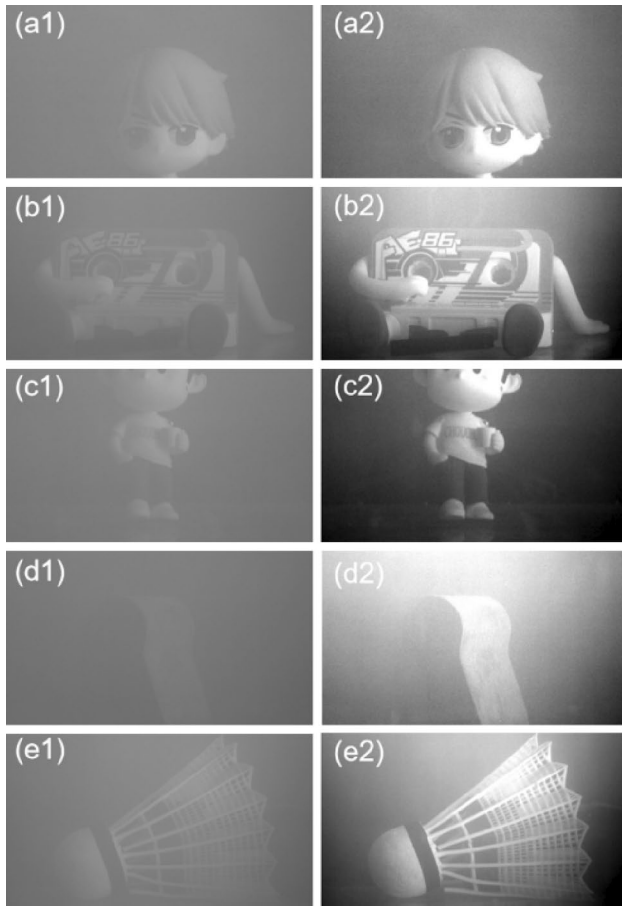


Fig. 8 a1, b1, c1, d1, and e1 are the original images affected by scattered light. a2, b2, c2, d2, and e2 are the images processed using the method of this paper

Table 2 Comparison of image quality metrics

	a1	a2	b1	b2	c1	c2	d1	d2	e1	e2
Contrast	0.3564	0.7789	0.2167	0.7057	0.2308	0.8021	0.1328	0.7347	0.2813	0.8889
Information entropy	5.0460	6.8395	5.3938	7.8084	5.1035	7.2823	4.7474	7.5353	5.6551	7.7817
Standard deviation	14.172	54.098	11.220	64.132	9.7001	47.935	9.3871	67.521	11.852	63.976

To further verify the imaging capability of the proposed technique for targets with different polarization degrees, different materials were selected for underwater imaging experiments, and the results are shown in Fig. 8. In Fig. 8e1, for example, the badminton ball is affected by the strong scattering of light waves, and the detail information is not easy to distinguish, while in Fig. 8b2, the detail information of the badminton ball is clearer after the algorithm is recovered. In Fig. 8c1, the pattern on the clothes of the doll is affected by scattering, and almost no information can be seen, but the pattern of the figure in Fig. 8c2 after recovery is visible, and the other images in Fig. 8 have similar effects. To objectively evaluate the image quality, as shown in Table 2, we calculated the contrast, information entropy, and standard deviation of each group of images in Fig. 8. As can be seen from the table, the quality indexes of each group of images have been significantly improved, which reflects the effectiveness of the algorithm and fully proves the general applicability of the method for imaging targets with different materials.

To verify the effectiveness of the algorithm in different concentrations of turbid water, turbid underwater environments with relatively low concentrations of fat milk solution (2.15 g/L) and high concentrations of fat milk solution (3.25 g/L) were set up, respectively. The experimental results are shown in Fig. 9. In the middle- and high-concentration turbid underwater, the detailed information of the image is buried, and the polarization difference-based underwater image restoration method can effectively remove the background scattered light and restore the detailed information of the target. To evaluate the image quality more comprehensively, in Table 3, we calculate the contrast, information entropy, and standard deviation of each image in Fig. 9. From Table 3, we can see that all the indexes of the images processed by our method are better than the original images, which indicates that our method can improve the clarity of underwater images under different turbid conditions.

Conclusion

In this paper, an improved polarization differential imaging method is proposed for the problem of poor effectiveness and real-time performance of the traditional polarization differential technique in the underwater imaging

process. Compared with the traditional polarization

Fig. 9 a11, b11, a21, and b21 are light intensity maps of different targets in medium- and high-concentration scattering media, respectively. a12, b12, a22 and b22 are images processed with the method herein

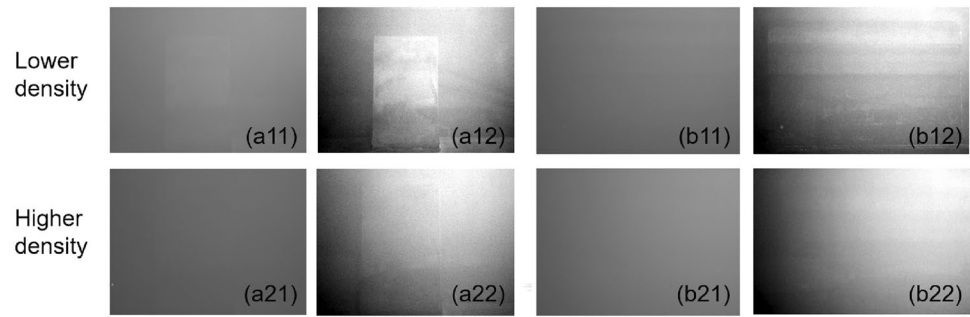


Table 3 Comparison of image quality metrics for different levels of turbidity

	Lower density				Higher density			
	a11	a12	b11	b12	a21	a22	b21	b22
Contrast	0.1491	0.8149	0.1901	0.9318	0.1345	0.7324	0.1829	0.8603
Information entropy	5.7191	7.8978	5.6011	7.8816	5.6011	7.847	5.3241	7.6433
Standard deviation	14.100	67.938	14.373	64.191	12.780	64.532	13.606	62.843

imaging method, the method in this paper uses the polarization angle of the background scattered light to select the best two mutually orthogonal polarization directions for the difference, which effectively improves the contrast and details of the image. The experimental results show that compared with the traditional polarization differential imaging method, the method in this paper has better effectiveness and real-time performance and can effectively improve the image quality of the strong scattering underwater environment.

The research in this paper has certain theoretical and practical significance. Theoretically, this paper proposes a new underwater polarization imaging method based on the polarization difference technique, which uses the polarization angle of the background scattered light to select the best polarization direction, which improves the contrast and details of the image, thus making the imaging effect of underwater detection more ideal. In practical application, the method in this paper also has high practicability and feasibility and can be applied to underwater detection, marine resources investigation, underwater archaeology, and other fields, which provides certain references and references for the development and application of underwater imaging technology.

In general, the research results of this paper have high academic value and practical significance and provide new ideas and methods for the development of underwater imaging technology. However, there are some shortcomings in the research of this paper, such as the small sample size of experimental data, the experimental environment control is not strict enough, and other problems, which need to be further improved and perfected in future research.

Acknowledgement This study was supported by the National Natural Science Foundation of China and the Key Research Project of Higher Education Institutions in Henan Province, "Research on the Clarification Technique of Underwater Polarized Images of Natural Water Bodies", under Grant Nos. 51609086 and 22A510015, respectively.

Declarations

Conflict of interest The authors declare that they have no known competing financial interests or personal relationships that could have appeared to influence the work reported in this paper.

References

1. F. Liu, S. Sun, P. Han, K. Yang, X. Shao, Development of underwater polarization image technology. *Laser Optoelectron. Prog.* **58**(06), 9–26 (2021)
2. B.A. Swartz, J.D. Cummings, Laser range-gated underwater imaging including polarization discrimination. in *Proc. SPIE 1537, underwater imaging, photography, and visibility* (1 December 1991)
3. C.S. Tan, G. Seet, A. Sluzek, X. Wang, C.T. Yuen, C.Y. Fam, H.Y. Wong, Scattering noise estimation of range-gated imaging system in turbid condition. *Opt. Express* **18**, 21147–21154 (2010)
4. W. Hou, E. Jarosz, S. Woods, W. Goode, A. Weidemann, Impacts of underwater turbulence on acoustical and optical signals and their linkage. *Opt. Express* **21**, 4367–4375 (2013)
5. E. Quevedo, E. Delory, G.M. Callicó, F. Tobajas, R. Sarmiento, Underwater video enhancement using multi-camera super-resolution. *Opt. Commun.* **404**, 94–102 (2017). (ISSN 0030-4018)
6. Y.Z. Li, C.J. Deng, W.L. Gong et al., Polarization difference Ghost imaging in turbid medium. *Acta Optica Sinica* **41**(15), 8 (2021)
7. H. Haofeng, L. Jiaqi, L. Xiaobo, L. Tiegeng, Underwater polarization difference imaging with three degrees of freedom. *Acta Optica Sinica* **41**(03), 222–227 (2021)
8. Y.Y. Schechner, S.G. Narasimhan, S.K. Nayar, Polarization-based vision through haze. *Appl. Opt.* **42**, 511–525 (2003)

9. Z. Jingping, D. Jinxin, L. Haoxiang, G. Fengqi, H. Xun, Development and polarization differential imaging in turbid media (Invited). *Electro-Opt. Technol. Appl.* **37**(05), 1–9 (2022)
10. M.P. Rowe, E.N. Pugh, J.S. Tyo, N. Engheta, Polarization-difference imaging: a biologically inspired technique for observation through scattering media. *Opt. Lett.* **20**, 608–610 (1995)
11. H. Pingli, *Underwater Targets Detection Based on Polarization Imaging* (Xidian University, Xi'An, 2018)
12. G.G. Stokes, On the change of refrangibility of light. *Philos. Trans. R. Soc.* **142**, 463–562 (1852)
13. Mu. Tingkui, D. Bao, F. Han, Y. Sun, Z. Chen, Q. Tang, C. Zhang, Optimized design, calibration, and validation of an achromatic snapshot full-Stokes imaging polarimeter. *Opt. Express* **27**, 23009–23028 (2019)
14. Z. Suying, Study on the improvement of extinction ratio in bias-preserving fiber coupling. University of Electronic Science and Technology of China (2007)
15. J. Xiaohua, Z. Chunmin, Z. Baohui, Z. Baochang, D. Juan, A new method for polarization detection using a polarization interferometric imaging spectrometer. *Acta Physica Sinica* **57**(12), 7565–7570 (2008)
16. E. Collett, W. Bellingham, E. Collett, The stokes polarization parameters. *Polariz. Light: Fundam. Appl.* 33–66 (2005)
17. M.I. Mishchenko, J.W. Hovenier, Depolarization of light backscattered by randomly oriented nonspherical particles. *Opt. Lett.* **20**, 1356–1358 (1995)
18. J. Guan, M. Ma, P. Sun, Optimization of rotating orthogonal polarization imaging in turbid media via the Mueller matrix. *Opt. Lasers Eng.* **121**, 104–111 (2019). (ISSN 0143-8166)
19. L. Yang, J. Liang, W. Zhang, J. Haijuan, L. Ren, X. Shao, Underwater polarimetric imaging for visibility enhancement utilizing active unpolarized illumination. *Opt. Commun.* **438**, 96–101 (2019). (ISSN 0030-4018)
20. J. Guan, J. Zhu, H. Tian et al., A study of real-time polarization differential underwater imaging based on Stokes vectors. *Acta Physica Sinica* **64**(22), 141–147 (2015)
21. X. Li, H. Hu, L. Zhao et al., Polarimetric image recovery method combining histogram stretching for underwater imaging. *Sci. Rep.* **8**, 12430 (2018)

Publisher's Note Springer Nature remains neutral with regard to jurisdictional claims in published maps and institutional affiliations.

Springer Nature or its licensor (e.g. a society or other partner) holds exclusive rights to this article under a publishing agreement with the author(s) or other rightsholder(s); author self-archiving of the accepted manuscript version of this article is solely governed by the terms of such publishing agreement and applicable law.